J. Phys. Chem. A **2000,** *104,* 7672−7678

Energy Barriers for Alkaline Hydrolysis of Carboxylic Acid Esters in Aqueous Solution by Reaction Field Calculations

Chang-Guo Zhan,*,†,# Donald W. Landry,*,† and Rick L. Ornstein‡

Department of Medicine, College of Physician & Surgeons, Columbia University,
New York, New York 10032 and the Pacific Northwest National Laboratory, Battelle-Northwest,
Environmental Technology Division, Mailstop K2-21, Richland, Washington 99352

Received: April 17, 2000

The hydrolysis of six representative alkyl esters in aqueous solution were evaluated by performing ab initio molecular orbital calculations using five different self-consistent reaction field (SCRF) procedures. Energy barriers were obtained for hydrolysis by bimolecular base-catalyzed acyl-oxygen cleavage ($B_{AC}2$) and bimolecular base-catalyzed alkyl-oxygen cleavage ($B_{AL}2$). Despite strong solute−solvent hydrogen bonding, the calculated solvent shifts of the energy barriers are dominated by electrostatic interactions between solute and solvent, and nonelectrostatic interactions largely cancel out. SCRF calculations that ignore volume polarization or use a charge renormalization scheme usually overestimate the solvent shifts of the energy barriers. A recently developed surface and volume polarization for electrostatic interaction (SVPE) procedure yields results comparable to experimental data when the solute cavity surface is defined as the 0.002 au electron charge isodensity contour. The differences between values from the SVPE calculations with this contour and the corresponding average experimental values for the examined esters are smaller than the range of experimental values reported by different laboratories. The SVPE calculations for the $B_{AC}2$ hydrolysis predicted the lowest energy barrier for methyl formate and the highest for *tert*-butyl acetate, and the remaining four esters grouped closely. These results are consistent with the substituent shifts of the experimental activation energies. The energy barriers predicted for $B_{AL}2$ hydrolysis are always considerably higher than those predicted for the $B_{AC}2$, consistent with the observation that in aqueous solution $B_{AL}2$ hydrolysis is negligible compared to $B_{AC}2$ for alkyl esters.

Introduction

The hydrolysis of carboxylic acid esters is one of the most thoroughly studied chemical reactions in chemistry and biochemistry.[1−3] A variety of experimental and theoretical studies[4−16] on ester hydrolysis have provided critical insights into the fundamental reaction mechanisms. Besides extensive interests within chemistry, the mechanism of base-catalyzed hydrolysis of esters figures prominently in many biological processes,[3d,17] such as the metabolism of the neurotransmitter acetylcholine and the degradation of cocaine. Applications include the design of transition-state analogues that inhibit acetylcholinesterase[18] and that elicit anti-cocaine catalytic antibodies.[19]

As is well-known, ester hydrolysis ($RCOOR' + H_2O \rightarrow RCOOH + R'OH$) involves cleavage of either the acyl-oxygen or alkyl-oxygen bond.[3c] The mode of cleavage may be determined by isotopic labeling and by stereochemical studies. Both types of cleavage are observed with acid or base catalysis and the result is a rich array of possible reaction mechanisms. We will focus only on the most common mechanisms involving specific base-catalyzed hydrolysis, i.e., hydroxide ion-catalyzed hydrolysis ($RCOOR' + HO^- \rightarrow RCOO^- + R'OH$ followed by $RCOO^- + H_2O \rightarrow RCOOH + HO^-$).[3c] The base-catalyzed hydrolysis of the majority of common alkyl esters occurs by the attack of hydroxide ion at the carbonyl carbon. This mode of hydrolysis has been designated as $B_{AC}2$ (base-catalyzed, acyl-oxygen cleavage, bimolecular),[3c] and is believed to occur by a two-step mechanism.[3] However, a concerted pathway can arise in the case of esters containing very good leaving groups (corresponding to a low pK_a value for R′OH).[8] The generally accepted two-step mechanism consists of the formation of a tetrahedral intermediate (first step), followed by decomposition of the tetrahedral intermediate to products $RCOO^- + R'OH$ (second step).[3c] The first step is usually rate-determining for the hydrolysis of alkyl esters in solution,[3c,8g] whereas the second step can be rate-determining in gas phase. Finally, a less common mode of ester hydrolysis, $B_{AL}2$ (base-catalyzed, alkyl-oxygen cleavage, bimolecular),[3c] competes with the $B_{AC}2$ mode. The $B_{AL}2$ mode, which leads to the same products as the $B_{AC}2$ process, is essentially an S_N2 substitution with a carboxylate leaving group (see Scheme 1).[3c]

Reaction pathways and energy barriers for both the $B_{AC}2$ and $B_{AL}2$ modes of hydrolysis of representative alkyl esters have been studied theoretically in the gas phase.[15] The highest energy barrier calculated for the $B_{AC}2$ process is always lower than the barrier for the $B_{AL}2$ process. The difference between the barrier for the $B_{AL}2$ process and the highest barrier for the $B_{AC}2$ process is only about 1−3 kcal/mol for the methyl esters, but becomes much larger for the others. The calculated results are all in good agreement with available experimental data in the gas phase.

It is more interesting to determine and compare energy barriers for the $B_{AC}2$ and $B_{AL}2$ modes of hydrolysis in aqueous

---

[†] Columbia University.

[#] Currently visiting at Pacific Northwest National Laboratory. E-mail: Chang-Guo.Zhan@pnl.gov.

[‡] Pacific Northwest National Laboratory.

10.1021/jp001459i CCC: $19.00

SCHEME 1

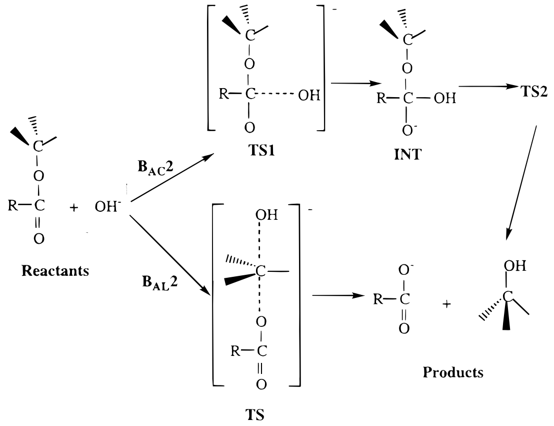

solution, since most of the ester hydrolysis processes in chemistry and biochemistry take place in aqueous solution. Obviously, reliable theoretical prediction of the energy barriers for the ester hydrolysis in solution should properly account for solvent effects. Sherer, Turner and Shields et al.[13] carried out semiempirical molecular orbital calculations on the first step of the $B_{AC}2$ mode, i.e., the formation of the tetrahedral intermediate. Employing Cramer and Truhlar's SM3 continuum solvation model[21] together with the PM3 molecular orbital method, they evaluated the energy barrier for the first step of the base-catalyzed hydrolysis of methyl acetate in aqueous solution as 19.8 kcal/mol as compared to an experimental activation energy of 10.45 kcal/mol in aqueous solution.[22] In addition, they found no significant difference between the calculated transition-state structures in gas phase and in solution. Haeffner et al.[11f] recently examined the solvent effects on the $B_{AC}2$ and $B_{AL}2$ modes of hydrolysis of methyl acetate at the MP2/6-31+G(d)//HF/6-31+G(d) level of theory. However, their transition-state structure for the first step (rate-determining step) of the $B_{AC}2$ mode was simply determined by a partial optimization with the constraint of the distance between the carbonyl carbon and the hydroxide oxygen, while the transition-state structure for the $B_{AL}2$ mode was fully optimized. Thus, the relative magnitudes of the energy barriers for the $B_{AC}2$ and $B_{AL}2$ mechanisms in aqueous solution still remain to be compared at the same level of theory.

Most recently, we determined reaction pathways and energy barriers for both steps of the $B_{AC}2$ hydrolysis of methyl acetate and methyl formate in aqueous solution using a hybrid supermolecule-polarizable continuum.[16] In this approach a few solvent water molecules with hydrogen bonds to solute are explicitly included and the remaining solvent water is modeled as a polarizable dielectric continuum. It was found that the lowest energy pathway involves a water-assisted proton transfer in the second step, i.e., the decomposition of the tetrahedral intermediate. It is this direct participation of solvent water in the proton transfer that significantly decreases the energy barrier for the decomposition of the tetrahedral intermediate such that the first step, i.e., the formation of the tetrahedral intermediate, becomes rate-determining in aqueous solution.[16] Calculations at various levels of theory also indicate that the energy barriers calculated for the supermolecular reaction systems, which are weakly interacting systems, are much more sensitive to the employed basis set than those for the corresponding water-free systems.[16] The energy barrier calculated at the MP2/6-311++G(3d, 2p) level of theory for the first step of the hydrolysis is in good agreement with the corresponding experimental activation energy. However, it is difficult to perform such a high level of ab initio theory on the supermolecular reaction systems associated with large ester molecules, such as cocaine. Thus, it is interesting to explore the feasibility of other computational strategies, such as those based on the pure dielectric continuum theory,[23] to predict the energy barriers for hydrolysis of large esters in aqueous solution.

We attempt herein to quantitatively determine the energy barriers for both the $B_{AC}2$ and $B_{AL}2$ modes of hydrolysis of six representative alkyl esters in aqueous solution by carrying out a series of self-consistent reaction field (SCRF) calculations. We are interested in both the solvent and substituent effects on the energy barriers. A variety of SCRF procedures were performed to evaluate the solvent shifts of the energy barriers. Comparison of the results determined by different SCRF calculations can provide insight into the dominant factors affecting solvent shifts, and comparison of the calculated energy barriers with available experimental activation data would validate different SCRF calculations.

Calculation Methods

Five different SCRF procedures were employed in the solvation calculations on the reactants and transition states to evaluate energy barriers for the ester hydrolysis in aqueous solution. The first three SCRF procedures employed are the standard polarizable continuum model (PCM),[24] the integral equation formalism for the polarizable continuum model (IEF-PCM),[25] and the conductor-like screening solvation model (COSMO)[26] implemented recently in the Gaussian98 program.[27] For these three SCRF procedures, the solute cavity surface is defined as overlapped spheres centered at the solute nuclei, and the contributions of short-range nonelectrostatic interactions, including cavitation, dispersion and Pauli repulsion, to the energy are also empirically estimated. Besides, these methods employ one of four available charge renormalization schemes for the surface polarization charge distribution to formally correct the deviation of the actually calculated total polarization charge from the ideal total polarization charge expected from Gauss' Law for the exact solution of Poisson's equation.[23] Obviously, in addition to the employed number of surface nodes (or tesserae) determining the accuracy of the numerical computation, the final results obtained from using these methods depend on many other choices, including the employed radii of the spheres at solute nuclei, the employed charge renormalization scheme, and the employed parameters for the short-range nonelectrostatic interactions. All the PCM, IEFPCM and COSMO calculations in this study were performed by using the default choices of the Gaussian98 program for the recommended standard parameters.

A fourth SCRF procedure employed in this work determines both surface and volume polarizations and is called the surface and volume polarization for electrostatic interaction (SVPE) model.[28,29] The final SCRF procedure used determines only the commonly treated surface polarization for the purpose of comparison, and may be called the surface polarization for electrostatic interaction (SPE) model.[28] Because no charge renormalization scheme was used in the SPE calculations, the differences between the SVPE and SPE results quantitatively represent the effects of volume polarization produced by the solute electron charge distribution outside the solute cavity. Both the SVPE and SPE procedures were developed and implemented recently in the GAMESS program[30] by one of us (together with Bentley and Chipman).[28a] Since the solute cavity surface is defined as a solute electron charge isodensity contour determined self-consistently during the SCRF iteration processes,[28] the SVPE results (converged to the exact solution of the Poisson's equation with a given numerical tolerance) and the corresponding SPE results depend only on the value of the contour for a given dielectric constant under a particular quantum chemical calculation level.[28a,d] This single parameter value has been calibrated as ∼0.001 au,[28b] by seeking the best overall agreement with experimental conformational free energy differences (62 experimental observations) in various polar solutes existing in various solvents. So, the 0.001 au contour was used in this study. Additional SVPE calculations with the 0.002 au contour were also performed to test the contour dependence of the SVPE results.

Regardless of the difference in the definitions of solute cavity surface, an advantage of the SVPE method compared to the PCM, IEFPCM and COSMO methods is the accurate determination of the volume polarization effects. A disadvantage is that the contributions of the short-range nonelectrostatic interactions to the solvent shift have not yet been evaluated. It follows that the best estimate of the solvent shift obtained from these standard reaction field calculations should be the sum of the solvent shift, ΔG(SVPE) including only the long-range electrostatic interaction contribution, calculated by the SVPE method, and the total nonelectrostatic interaction contribution, $\Delta G_{\mathrm{non-elec}}$, determined by the PCM, IEFPCM or COSMO method. Actually, the PCM, IEFPCM and COSMO methods implemented in Gaussian98 employ the same procedure and the same set of parameters in the determination of the nonelectrostatic interactions, and therefore lead to the same results for $\Delta G_{\mathrm{non-elec}}$. Nevertheless, the contributions of the nonelectrostatic interactions to the energy changes during the reaction process are expected to be largely canceled out, for the same reason that the contributions of the nonelectrostatic interactions to the conformational free energy difference could, as examined previously.[28b] This expectation can be examined quantitatively by evaluating the changes of $\Delta G_{\mathrm{non-elec}}$.

All the SCRF calculations in this study were performed at the level of second-order MØller−Plesset (MP2) theory with the 6-31++G(d,p) basis set by using the geometries optimized at the B3LYP/6-31++G(d,p) level of theory[31] in gas phase. The energy barriers calculated previously for the base-catalyzed hydrolysis of alkyl esters in gas phase[15] indicate that the MP2/6-31++G(d,p)//B3LYP/6-31++G(d,p) results are almost identical to the corresponding MP2/6-31++G(d,p)//MP2/6-31++G(d,p) results, and that the energy calculations at the MP2/6-31++G(d,p) level of theory are adequate for studying the energy profile of the hydrolysis. Replacing the MP2 method with the QCISD(T) method, while holding constant the basis set, did not significantly change the results. For the energy barriers, the largest difference between the MP2/6-31++G(d,p)//B3LYP/6-31++G(d,p) and the MP2/6-31++G(d,p)//MP2/6-31++G(d,p) results is 0.2 kcal/mol, and the largest difference between the MP2/6-31++G(d,p)//B3LYP/6-31++G(d,p) and the QCISD(T)/6-31++G(d,p)//MP2/6-31++G(d,p) results is 0.3 kcal/mol.[15] Hence, in this study, the geometries optimized at the B3LYP/6-31++G(d,p) level in gas phase were employed to carry out various SCRF solvation calculations at the MP2/6-31++G(d,p) level. For all the SCRF calculations at the MP2/6-31++G(d,p) level, the MP2 perturbation procedure was performed for electron correlation correction after the converged Hartree−Fock (HF) wave function of solute in reaction field is obtained. The dielectric constant of water used in this study is 78.5.

Unless indicated otherwise, the Gaussian94[32] and Gaussian98[27] programs were used to obtain the present results. All the computations in this work were performed on Silicon Graphics, Inc. Origin 200 multiprocessor computers.

TABLE 1: Energy Barriers (kcal/mol) Determined by Various SCRF Calculations for the Ester Hydrolysis via the $B_{AC}2$ Route in Aqueous Solution Compared with Available Experimental Activation Energies

solvation calculations methods[a]	barriers for ester hydrolysis via $B_{AC}2^{e}$					
	a	**b**[k]	**c**	**d**	**e**	**f**
$\Delta G(\mathrm{SVPE\text{-}HF})_{\mathrm{elec}}{}^{b}$	7.3	5.5	6.3	6.7	7.7	11.7
$\Delta G(\mathrm{SVPE\text{-}MP2})_{\mathrm{elec}}$	7.2	5.4	6.3	6.6	7.5	11.6
$\Delta G(\mathrm{SPE\text{-}HF})_{\mathrm{elec}}{}^{b}$	11.8	9.4	14.2	12.6	14.4	18.9
$\Delta G(\mathrm{SPE\text{-}MP2})_{\mathrm{elec}}$	11.7	9.2	14.1	12.5	14.2	18.7
$\Delta G(\mathrm{SVPE\text{-}HF,0.002})_{\mathrm{elec}}{}^{b,c}$	10.6	8.1	9.9	9.8	10.9	15.2
$\Delta G(\mathrm{SVPE\text{-}MP2,0.002})_{\mathrm{elec}}{}^{c}$	10.4	7.9	9.7	9.6	10.7	14.9
$\Delta G_{\mathrm{non-elec}}{}^{d}$	0.5	0.7	1.1	0.6	0.7	0.8
$\Delta G(\mathrm{SVPE\text{-}HF})_{\mathrm{elec}} + \Delta G_{\mathrm{non-elec}}$	7.7	6.3	7.4	7.3	8.4	12.5
$\Delta G(\mathrm{SVPE\text{-}MP2})_{\mathrm{elec}} + \Delta G_{\mathrm{non-elec}}$	7.7	6.1	7.4	7.2	8.2	12.4
$\Delta G(\mathrm{SPE\text{-}HF})_{\mathrm{elec}} + \Delta G_{\mathrm{non-elec}}$	12.2	10.1	15.3	13.2	15.1	19.7
$\Delta G(\mathrm{SPE\text{-}MP2})_{\mathrm{elec}} + \Delta G_{\mathrm{non-elec}}$	12.1	10.0	15.2	13.1	14.9	19.5
$\Delta G(\mathrm{SVPE\text{-}HF,0.002})_{\mathrm{elec}} + \Delta G_{\mathrm{non-elec}}$	11.1	8.9	11.1	10.4	11.6	16.0
$\Delta G(\mathrm{SVPE\text{-}MP2,0.002})_{\mathrm{elec}} + \Delta G_{\mathrm{non-elec}}$	10.9	8.6	10.9	10.2	11.3	15.7
$\Delta G(\mathrm{PCM\text{-}HF})^{b}$	11.8	12.4	16.3	16.9	17.2	21.9
$\Delta G(\mathrm{PCM\text{-}MP2})$	10.7	11.0	14.5	15.4	15.3	19.9
$\Delta G(\mathrm{IEFPCM\text{-}HF})^{b}$	12.5	10.9	16.0	15.7	16.2	20.3
$\Delta G(\mathrm{IEFPCM\text{-}MP2})$	11.0	9.5	14.2	14.1	14.3	18.3
$\Delta G(\mathrm{COSMO{-}HF})^{b}$	17.4	15.6	20.5	21.2	21.4	25.7
$\Delta G(\mathrm{COSMO\text{-}MP2})$	15.7	13.9	18.4	19.4	19.3	23.4
exp(pure water)	10.45[f]	9.81[g]				
exp(20.00% acetone in water)[h]				10.95		
exp(33.75% acetone in water)[h]				10.38		
exp(51.00% acetone in water)[h]				10.22		
exp(62% acetone in water)[i]				9.80		
exp(62% acetone in water)[j]	12.20			12.00	12.20	14.30

[a] All calculations were carried out with the 6-31++G(d,p) basis set by employing geometries optimized at the B3LYP/6-31++G(d,p) level in gas phase. ZPVE corrections determined by the B3LYP calculations in gas phase are included for all the energy barriers. [b] The SCRF calculations were performed with HF method. The energy barrier is taken as the sum of the energy difference evaluated in gas phase at the MP2/6-31++G(d,p) level and the corresponding solvent shift determined by the SCRF calculations at the HF/6-31++G(d,p) level. [c] The SVPE calculations used the 0.002 au contour, instead of the 0.001 au contour used in the others SVPE and SPE calculations. [d] The total contribution of nonelectrostatic interactions to the energy barrier determined by the PCM calculations. Actually, the corresponding IEFPCM and COSMO calculations gave exactly the same $\Delta G_{\mathrm{non-elec}}$ values. [e] The esters: **a** CH_3COOCH_3; **b** $HCOOCH_3$; **c** $C_6H_5COOCH_3$; **d** $CH_3COOCH_2CH_3$; **e** $CH_3COOCH(CH_3)_2$; **f** $CH_3COOC(CH_3)_3$. [f] Experimental activation energy from ref 22. [g] Experimental enthalpy of activation from ref 33. [h] Experimental activation energy from ref 34 (The temperature range: 15.87−26.10 °C). [i] Experimental activation energy from ref 35. [j] Experimental activation energy from ref 36. [k] The enthalpy of activation (calculated by including the thermal correction to enthalpy instead of the ZPVE correction to energy) is ∼0.1 kcal/mol smaller than the corresponding energy barrier.

Results and Discussion

$B_{AC}2$ Mode of Hydrolysis. Summarized in Table 1 are the energy barriers determined by the MP2/6-31++G(d,p) calculations with various SCRF procedures for the $B_{AC}2$ hydrolysis of six representative alkyl esters in aqueous solution compared with available experimental activation energies. The energy barrier for the $B_{AC}2$ hydrolysis is the energy change from the individual solvated reactants, RCOOR′ + HO^-, to the solvated first transition state, since the first step is rate-determining. The energy barrier for the $B_{AL}2$ process is the energy change from the individual solvated reactants, RCOOR′ + HO^-, to the solvated transition state. To examine the electron correlation effects on the solvent shifts, the energy barriers based on the solvent shifts determined by the corresponding HF calculations are also listed in Table 1 for comparison. The results listed in Table 1 indicate that electron correlation effects on the solvent shifts determined by the SVPE and SPE calculations are all very small. The largest difference between the solvent shifts calculated at the HF/6-31++G(d,p) level and those at the MP2/6-31++G(d,p) level is 0.3 kcal/mol. The differences between solvent shifts evaluated at the HF/6-31++G(d,p) level and those at the MP2/6-31++G(d,p) level are 1.1−2.0 kcal/mol for the PCM calculations, 1.4−2.0 kcal/mol for the IEFPCM calculations, and 1.7−2.3 kcal/mol for the COSMO calculations.

We sought to compare the calculated results with available experimental data. The experimental activation data in pure water are available only to methyl acetate and methyl formate (Table 1). For ethyl acetate, three laboratories reported experimental activation energies in various aqueous acetone solutions. The values 9.80 and 12.00 kcal/mol reported for ethyl acetate with the same solvent (62% acetone in water) by different laboratories[35,36] illustrate the possible systematic deviations for experimental data. The values for ethyl acetate in different solutions from a same laboratory[34] suggest that the activation energy decreases with increasing the concentration of acetone in water. Clearly, plausible substituent shifts of the activation energy must be derived from the experimental data in the same kind of aqueous solution reported by the same laboratory.[36]

Compared to available experimental activation energies collected in Table 1, the SVPE calculations with the previously calibrated 0.001 au contour (default) systematically underestimate the energy barriers, although the calculated energy barriers adequately reflect an important trend for the substituent shifts of the experimental activation energies. According to the experimental activation energies determined in the same laboratory[36] for the four alkyl acetates considered here, changing the leaving group OR′ from $R' = CH_3$ to $R' = CH_2CH_3$ and to $R' = CH(CH_3)_2$ does not significantly change the first energy barrier. However, changing OR′ from $R' = CH(CH_3)_2$ to $R' = C(CH_3)_3$ increases the first energy barrier by 2.1 kcal/mol. The systematic deviation of the calculated energy barriers from the experimental activation energies may be attributed to the effects of the solute−solvent hydrogen bonding,[16] because this interaction is not explicitly included in the SCRF calculations. For systems with strong hydrogen bonding between solute and solvent molecules, the contributions of the short-range nonelectrostatic interactions to the energy barriers might be more important, or/and the electrostatic interactions might become stronger than those expected for the systems without solute−solvent hydrogen bonding.

To evaluate the solute−solvent hydrogen bonding effects, we first examined the nonelectrostatic interactions not considered in the SVPE calculations. As listed in Table 1, the total contributions of the nonelectrostatic interactions, $\Delta G_{\text{non-elec}}$, to the energy barriers determined by the PCM calculations are 0.5−1.1 kcal/mol. Adding the $\Delta G_{\text{non-elec}}$ values to the corresponding SVPE results, the calculated energy barriers are slightly closer to the experimental data. It follows that the total contributions of the nonelectrostatic interactions to the energy barriers are largely canceled out, and this neglect is not a major factor in deviations of the calculated energy barriers from the corresponding experimental data. The dominant factor might be that the SVPE calculations with the 0.001 au contour significantly underestimate the solute−solvent electrostatic interactions in the base-catalyzed hydrolysis systems involving strong solute−solvent hydrogen bonds. With solute−solvent hydrogen bonding, the average distance between solute and solvent molecules should be slightly shorter than that without the hydrogen bonding. Therefore, the solute cavity sizes used in the SCRF calculations on the systems involving solute−solvent hydrogen bonding should be slightly smaller, and should be associated with a slightly larger contour value. For this reason, the 0.002 au contour was also tested in the SVPE calculations. As seen in Table 1, the energy barriers determined by the SVPE calculations with the 0.002 au contour are in good agreement with the available experimental activation energies. Further adding the contributions of the nonelectrostatic interactions to the solvent shifts determined by the SVPE calculations with the 0.002 au contour, the calculated results become slightly closer to the corresponding experimental activation data. The energy barriers calculated for methyl acetate and ethyl acetate are all between the corresponding experimental activation energies reported by different laboratories. The average deviation of the calculated results from the corresponding experimental activation data reported for other three esters is ∼1.2 kcal/mol. The largest deviation is ∼1.4 kcal/mol. Thus, the SVPE calculations at 0.002 au contour are sufficient based on absolute comparability to experimental values for a given ester.

Concerning the relative magnitudes of the calculated energy barriers, the lowest energy barrier is associated with methyl formate, and the highest energy barrier is associated with *tert*-butyl acetate. The energy barriers associated with the other four esters are bunched closely. So, the trend for the substituent shifts of the experimental activation energies[36] mentioned above is well reproduced in the predicted energy barriers derived from the SVPE calculations with the 0.002 au contour.

We considered the energy barriers determined by other SCRF calculations. For each of the six esters examined in this study, the energy barrier determined by the COSMO calculations is always larger than those determined by the other SCRF calculations. Compared to available experimental activation energies, the COSMO calculations significantly overestimate the energy barriers for the five alkyl esters, especially for $CH_3COOC(CH_3)_3$. Chipman has recently demonstrated that the COSMO and IEFPCM procedures are equivalent for infinite dielectric constant when they are all performed without charge renormalization.[23f] Since water is a very high dielectric constant solvent, the significant differences between the COSMO results and IEFPCM results may be mainly attributed to the use of the different (default) charge renormalization schemes. For the COSMO calculations the calculated polarization charges on each tessera is scaled by a constant factor, whereas for the PCM and IEFPCM calculations the effect of outlying charge is accounted for by means of an additional charge distributed according to the solute electronic density.

Comparing the results determined by the SPE calculations with the corresponding SVPE results, one can see that the volume polarization effects on the energy barriers for the examined systems are 3.8−7.1 kcal/mol when the 0.001 au contour is used. The recently developed IEFPCM procedure may be regarded as a slightly improved version the PCM procedure by the same laboratory at Pisa. So, the energy barriers determined by the two kinds of SCRF calculations are very close to each other, and the IEFPCM results are slightly closer to the experimental activation energies and the results of the SVPE calculations with the 0.002 au contour than the corresponding PCM results. Regardless of the differences in technical details, the major differences of the SPE calculations from the PCM and IEFPCM calculations carried out in this study include (1) the solute cavity surface is defined as an electron charge isodensity contour, rather than overlapped spheres; (2) the charge renormalization, which may be regarded as an approximate consideration of the volume polarization, is not performed; and (3) the nonelectrostatic interactions are ignored. The results listed in Table 1 indicate that these differences do not dramatically affect the results calculated at the MP2/6-31++G(d,p) level, because the energy barriers determined by the SPE calculations (with the 0.001 au contour) are close to the corresponding barriers determined by the PCM and IEFPCM calculations, especially by the IEFPCM calculations. It implies that the significant differences between the SVPE results and the corresponding SPE, PCM and IEFPCM results are dominated by the different treatments of the volume polarization produced by the solute electron charge distribution outside the cavity. As seen in Table 1, for methyl acetate the energy barriers determined by the SPE, PCM and IEFPCM calculations are all in good agreement with the energy barrier determined by the SVPE calculations using the 0.002 au contour and with the available experimental values of the activation energy, 10.45 and 12.20 kcal/mol.[22,36] This means that the volume polarization and the solute−solvent hydrogen bonding effects on the energy barrier for methyl acetate are nearly canceled out. However, for other larger alkyl acetates the two kinds of effects cannot cancel out. This is because the volume polarization effects for a larger solute are usually stronger since the larger solute usually has greater charge outside the cavity, while the solute−solvent hydrogen bonding effects do not significantly change for the alkyl acetates examined. Changing the leaving group OR′ of the alkyl acetates, CH_3COOR', from $R' = CH_3$ to $R' = CH_2CH_3$, $R' = CH(CH_3)_2$, and $R' = C(CH_3)_3$, the energy barriers determined by the SPE calculations become gradually larger. The PCM and IEFPCM results are also similar to the SPE results, except for ethyl acetate. Thus, the SPE, PCM and IEFPCM calculations overestimate the energy barriers for other alkyl esters, while accidentally producing energy barriers close to the experimental activation energy for methyl acetate and methyl formate. Therefore, the SCRF calculations without accurate determination of the volume polarization cannot satisfactorily reproduce the experimental trends regarding the substituent effects on the energy barriers for the $B_{AC}2$ hydrolysis of the alkyl acetates.

$B_{AL}2$ Mode of Hydrolysis. Because the energy barriers determined for $B_{AC}2$ hydrolyses were adequately modeled by the SVPE with 0.002 au contour, the corresponding $B_{AL}2$ hydrolyses were similarly calculated (Table 2). The corresponding results calculated by the PCM, IEFPCM and COSMO methods are included for comparison. As seen in Table 2, the total contributions of the nonelectrostatic interactions, $\Delta G_{non-elec}$, to the energy barriers are within ∼0.4 kcal/mol. Concerning the relative magnitudes of the energy barriers, the lowest energy barrier for the $B_{AL}2$ mode of hydrolysis is also associated with methyl formate, as is for the $B_{AC}2$ mode of hydrolysis. The energy barriers for the other two methyl esters are close to each other, although the barrier for $C_6H_5COOCH_3$ is ∼1 kcal/mol higher than that for CH_3COOCH_3. When $R = CH_3$ and when $R' = CH_3$, CH_2CH_3, $CH(CH_3)_2$ and $C(CH_3)_3$, the predicted energy barriers are ∼22, ∼27, ∼29 and ∼38 kcal/mol, respectively. It follows that substitution of the α hydrogen in OR′ with a methyl group considerably increases the energy barrier for the $B_{AL}2$ process in aqueous solution. The similar trend was also found in the substituent shifts of the energy barrier predicted for the $B_{AL}2$ process in gas phase.[15] The energy barriers predicted for the $B_{AL}2$ mode of hydrolysis of CH_3COOCH_3, $HCOOCH_3$, $C_6H_5COOCH_3$, $CH_3COOCH_2CH_3$, $CH_3COOCH(CH_3)_2$ and $CH_3COOC(CH_3)_3$ in gas phase are ∼10, ∼9, ∼8, ∼13, ∼17 and ∼26 kcal/mol, respectively. So, the solvent shifts of the energy barriers for the $B_{AL}2$ process are in the range of 11−15 kcal/mol.

TABLE 2: Energy Barriers (kcal/mol) Determined by Various SCRF Calculations for the Ester Hydrolysis via $B_{AL}2$ Route in Aqueous Solution

methods for solvation calculations[a]	esters for hydrolysis via $B_{AL}2$[e]					
	a	**b**	**c**	**d**	**e**	**f**
$\Delta G(\text{SVPE-HF,0.002})_{elec}$[b,c]	21.7	19.2	22.9	26.1	29.3	37.5
$\Delta G(\text{SVPE-MP2,0.002})_{elec}$[c]	22.0	19.4	22.9	26.2	29.6	37.8
$\Delta G_{non-elec}$[d]	0.1	0.2	0.2	0.4	−0.4	−0.3
$\Delta G(\text{SVPE-HF,0.002})_{elec} + \Delta G_{non-elec}$	21.8	19.4	23.1	26.5	28.9	37.2
$\Delta G(\text{SVPE-MP2,0.002})_{elec} + \Delta G_{non-elec}$	22.1	19.6	23.1	26.6	29.2	37.5
$\Delta G(\text{PCM-HF})$[b]	27.7	22.5	22.8	29.9	44.9	54.4
$\Delta G(\text{PCM-MP2})$	26.9	21.4	21.9	29.0	43.2	52.7
$\Delta G(\text{IEFPCM-HF})$[b]	25.0	21.1	21.4	28.3	42.6	51.8
$\Delta G(\text{IEFPCM-MP2})$	24.2	20.1	20.5	27.4	41.1	50.2
$\Delta G(\text{COSMO−HF})$[b]	30.1	26.1	23.1	33.3	48.4	57.7
$\Delta G(\text{COSMO-MP2})$	29.0	24.8	25.0	32.2	46.6	55.8

[a] All calculations were carried out with the 6-31++G(d,p) basis set by employing geometries optimized at the B3LYP/6-31++G(d,p) level in gas phase. ZPVE corrections determined by the B3LYP calculations in gas phase are included for all energy barriers. [b] The SCRF calculations were performed with HF method. The energy barrier is taken as the sum of the energy difference evaluated in gas phase at the MP2/6-31++G(d,p) level and the corresponding solvent shift determined by the SCRF calculations at the HF/6-31++G(d,p) level. [c] The SVPE calculations used the 0.002 au contour. [d] The total contribution of nonelectrostatic interactions to energy barrier determined by the PCM calculations. Actually, the corresponding IEFPCM and COSMO calculations gave exactly the same $\Delta G_{non-elec}$ values. [e] The esters: **a** CH_3COOCH_3; **b** $HCOOCH_3$; **c** $C_6H_5COOCH_3$; **d** $CH_3COOCH_2CH_3$; **e** $CH_3COOCH(CH_3)_2$; **f** $CH_3COOC(CH_3)_3$.

The energy barriers predicted for the $B_{AL}2$ process in aqueous solution are always considerably higher than the corresponding energy barriers predicted for the $B_{AC}2$ process. The difference in energy barrier between the two hydrolysis processes is 11−12 kcal/mol for the three methyl esters, ∼16 kcal/mol for $CH_3COOCH_2CH_3$, ∼18 kcal/mol for $CH_3COOCH(CH_3)_2$ and ∼22 kcal/mol for $CH_3COOC(CH_3)_3$. This is different from what is found for hydrolysis in gas phase.[15] For the hydrolysis in gas phase, the energy barriers calculated for $B_{AL}2$ process are only ∼1−3 kcal/mol higher than those for the corresponding $B_{AC}2$ process. These results indicate the basis for the observation that the $B_{AL}2$ process in aqueous solution is negligible compared to the corresponding $B_{AC}2$ process, although both the $B_{AC}2$ and $B_{AL}2$ processes are competitive in gas phase.

The differences between the energy barriers determined by the SVPE calculations and those by the PCM, IEFPCM and COSMO calculations for the $B_{AL}2$ process are similar to the differences found for the $B_{AC}2$ process. For example, the energy barriers determined by the PCM, IEFPCM and COSMO calculations are significantly larger than the corresponding SVPE results for all the esters, except for $C_6H_5COOCH_3$; the differences are usually smaller for the methyl esters, and become much larger for $CH_3COOCH(CH_3)_2$ and $CH_3COOC(CH_3)_3$; the IEFPCM results are slightly closer to the corresponding SVPE results than the PCM results; and the energy barriers determined by the COSMO calculations are always larger than the corresponding barriers determined by the other SCRF calculations. Nevertheless, regarding the relative importance of the $B_{AC}2$ and $B_{AL}2$ processes, all these SCRF calculations still lead to a qualitatively consistent conclusion that the energy barrier for the $B_{AL}2$ process is always considerably higher than that for the corresponding $B_{AC}2$ process in aqueous solution.

Conclusion

Five different SCRF procedures were employed to evaluate the energy barriers for both the $B_{AC}2$ and $B_{AL}2$ modes of hydrolysis of six representative alkyl esters in aqueous solution. The calculated results reveal that electron correlation effects on the solvent shifts of the energy barriers determined by the SVPE and SPE calculations are all very small. The differences between the solvent shifts calculated at the HF/6-31++G(d,p) level and those at the MP2/6-31++G(d,p) level are only 0.0−0.3 kcal/mol. The differences become slightly larger for the solvent shifts of the energy barriers determined by the other SCRF calculations in which the cavity surface is defined as the overlapped spheres.

Despite strong solute−solvent hydrogen bonding, the calculated solvent shifts of the energy barriers are dominated by the electrostatic interactions between solute and solvent. The contributions of the nonelectrostatic interactions to the energy barriers are largely canceled out, ranging from 0.1 to 1.1 kcal/mol. These results reveal that the key to success for solvation calculations is the accurate determination of the solute−solvent electrostatic interactions. SCRF calculations which ignore volume polarization or use a charge renormalization scheme usually overestimate the solvent shifts of the energy barriers. Although the SPE, PCM and IEFPCM calculations accidentally give energy barriers close to the experimental activation energies for the $B_{AC}2$ hydrolysis of methyl acetate and methyl formate, these calculations and COSMO calculations cannot satisfactorily reproduce the experimental trends for the substituent shifts of the $B_{AC}2$ energy barriers.

The recently developed SVPE procedure, which accurately determines both surface and volume polarizations, yields satisfactory results compared to experimental activation data when the solute cavity surface is defined by the 0.002 au electron charge isodensity contour of the solvated solute. The SVPE results can further be improved by adding the total contributions of the nonelectrostatic interactions estimated by the PCM method. The energy barriers calculated for methyl acetate and ethyl acetate fall within the range of experimental activation energies reported by different laboratories. The average deviation of the calculated results from the corresponding experimental activation data reported for other three esters is ∼1.2 kcal/mol. The largest deviation (∼1.4 kcal/mol for *tert*-butyl acetate) is smaller than the difference between the largest and smallest experimental values of the activation energy reported by different laboratories for ethyl acetate. The SVPE calculations with 0.002 au contour for the $B_{AC}2$ hydrolysis of the six esters predicted the lowest energy barrier for methyl formate and the highest for *tert*-butyl acetate. The energy barriers for the $B_{AC}2$ hydrolysis of the other four esters are very closely grouped. These results are consistent with the substituent shifts of the available experimental activation energies. Concerning the $B_{AL}2$ mode of hydrolysis, the lowest energy barrier is also associated with methyl formate. The energy barriers for the $B_{AL}2$ hydrolysis of the other two methyl esters are similar, and substitution of the α hydrogen in OR′ with a methyl group considerably increases the energy barrier.

The energy barriers determined by all the SCRF calculations for the $B_{AL}2$ process in aqueous solution are always significantly higher than the corresponding energy barriers predicted for the $B_{AC}2$ process. According to the results of the SVPE calculations with the 0.002 au contour, the difference in energy barrier between the two hydrolysis processes is 11−12 kcal/mol for the three methyl esters, ∼16 kcal/mol for $CH_3COOCH_2CH_3$, ∼18 kcal/mol for $CH_3COOCH(CH_3)_2$ and ∼22 kcal/mol for $CH_3COOC(CH_3)_3$. The calculated results indicate the basis for the observation that in aqueous solution the $B_{AL}2$ process is negligible compared to the corresponding $B_{AC}2$ process, although both the $B_{AC}2$ and $B_{AL}2$ hydrolyses of methyl esters are competitive in gas phase.

Acknowledgment. This work was supported by the Counterdrug Technology Assessment Center at the Office of National Drug Control Policy (D.W.L.).

References and Notes

(1) (a) Bender, M. L. *Chem. Rev.* **1960**, *60*, 53. (b) Johnson, S. L. *Adv. Phys. Org. Chem.* **1967**, *5*, 237. (c) Jencks, W. P. *Chem. Rev.* **1972**, *72*, 705.

(2) (a) Bamford, C. H., Tipper, C. F. H., Eds. *Ester Formation and Hydrolysis*; Elsevier: Amsterdam, 1972; Vol. 10. (b) Ingold, C. K. *Structure and Mechanism in Organic Chemistry*, 2nd ed.; Cornell University Press: Ithaca, New York, 1969; p 1131.

(3) (a) Jones, R. A. Y. *Physical and Mechanistic Organic Chemistry*; Cambridge University Press: Cambridge, U.K., 1979; p 227. (b) McMurry, J. *Organic Chemistry*, 2nd ed.; Cole Publishing: CA, 1988. (c) Lowry, T. H.; Richardson, K. S. *Mechanism and Theory in Organic Chemistry*, 3rd ed.; Harper and Row: New York, 1987. (d) Williams, A. In *Enzyme Mechanisms*; Page, M. I., Williams, A., Eds.; Burlington: London, 1987; p 123.

(4) (a) Polanyi, M.; Szabo, A. L. *Trans Faraday Soc.* **1934**, *30*, 508. (b) Bender, M. L.; Dewey, R. S. *J. Am. Chem. Soc.* **1956**, *78*, 317. (c) Samuel, D.; Silver, B. L. *Adv. Phys. Org. Chem.* **1965**, *3*, 123.

(5) (a) Bender, M. L.; Heck, H. d'A. *J. Am. Chem. Soc.* **1967**, *89*, 1211. (b) Shain, S. A.; Kirsch, J. F. *J. Am. Chem. Soc.* **1968**, *90*, 5848. (c) Rylander, P. N.; Tarbell, D. S. *J. Am. Chem. Soc.* **1950**, *72*, 3021. (d) Fukuda, E. K.; McIver, Jr. R. T. *J. Am. Chem. Soc.* **1979**, *101*, 2498.

(6) (a) Faigle, J. F. G.; Isolani, P. C.; Riveros, J. M. *J. Am. Chem. Soc.* **1976**, *98*, 2049. (b) Takashima, K.; Riveros, J. M. *J. Am. Chem. Soc.* **1978**, *100*, 6128. (c) Johlman, C. L.; Wilkins, C. L. *J. Am. Chem. Soc.* **1985**, *107*, 327. (d) Bender, M. L.; Thomas, R. J. *J. Am. Chem. Soc.* **1961**, *83*, 4189. (e) Bender, M. L.; Matsui, H.; Thomas, R. J.; Tobey, S. W. *J. Am. Chem. Soc.* **1961**, *83*, 4193. (f) Bender, M. L.; Heck, H., d'A. *J. Am. Chem. Soc.* **1967**, *89*, 1211. (g) Bender, M. L.; Ginger, R. D.; Unik, J. P. *J. Am. Chem. Soc.* **1958**, *80*, 1044. (h) O'Leary, M. H.; Marlier, J. F. *J. Am. Chem. Soc.* **1979**, *101*, 3300.

(7) Takashima, K.; Jose, S. M.; do Amaral, A. T.; Riveros, J. M. *J. Chem. Soc., Chem. Commun.* **1983**, 1255.

(8) (a) Ba−Saif, S. A.; Luthra, A. K.; Williams, A. *J. Am. Chem. Soc.* **1987**, *109*, 6362. (b) Luthra, A. K.; Ba-Saif, S. A.; Chrystiuk, E.; Williams, A. *Bull. Soc. Chim. Fr.* **1988**, 392. (c) Ba-Saif, S. A.; Luthra, A. K.; Williams, A. *J. Am. Chem. Soc.* **1989**, *111*, 2647. (d) Ba-Saif, S. A.; Waring, M. A.; Williams, A. *J. Am. Chem. Soc.* **1990**, *112*, 8115. (e) Guthrie, J. P. *J. Am. Chem. Soc.* **1991**, *113*, 3941. (f) Hengge, A. *J. Am. Chem. Soc.* **1992**, *114*, 6575. (g) Marlier, J. F. *J. Am. Chem. Soc.* **1993**, *115*, 5953.

(9) (a) Bunnett, J. F. *J. Am. Chem. Soc.* **1961**, *83*, 4978. (b) Rogers, G. A.; Bruice, T. C. *J. Am. Chem. Soc.* **1973**, *95*, 4452; **1974**, *96*, 2473; **1974**, *96*, 2481. (c) Gravitz, N.; Jencks, W. P. *J. Am. Chem. Soc.* **1974**, *96*, 489. (d) Capon, B.; Ghosh, K.; Grieve, D. M. A. *Acc. Chem. Res.* **1981**, *14*, 306. (e) McClelland, R. A.; Santry, L. J. *Acc. Chem. Res.* **1983**, *16*, 394.

(10) (a) Bowden, K. *Adv. Phys. Org. Chem.* **1993**, *28*, 171. (b) Bowden, K. *Chem. Soc. Rev.* **1995**, *25*, 431. (c) Bowden, K.; Byrne, J. M.. *J. Chem. Soc., Perkin Trans. 2* **1996**, 2203; **1997**, 123. (d) Bowden, K.; Izadi, J.; Powell, S. L. J. *Chem. Rev.* **1997**, *97*, 404. (e) Bowden, K.; Battah, S. *J. Chem. Soc., Perkin Trans. 2* **1998**, 1603. (f) Li, P.; Zhao, K.; Deng, S.; Landry, D. W. *Helv. Chim. Acta* **1999**, *82*, 85.

(11) (a) Dewar, M. J. S.; Storch, D. M. *J. Chem. Soc., Chem. Commun.* **1985**, *94*. (b) Dewar, M. J. S.; Storch, D. M. *J. Chem. Soc., Perkin Trans. 2* **1989**, 877. (c) Hori, K. *J. Chem. Soc., Perkin Trans. 2* **1992**, 1629. (d) Hori, K.; Kamimura, A.; Kimoto, J.; Gotoh, S.; Ihara, Y. *J. Chem. Soc., Perkin Trans. 2* **1994**, 2053. (e) Hori, K.; Kamimura, A.; Ando, K.; Nakao, Y.; Mizumura, M. *Tetrahedron.* **1994**, *53*, 2053. (f) Haeffner, F.; Hu, C.-H.; Brinck, T.; Norin, T. *J. Mol. Struct. (THEOCHEM)* **1999**, *459*, 85.

(12) (a) Williams, I. H.; Spangler, D.; Femec, D. A.; Maggiora, G. M.; Schowen, R. L. *J. Am. Chem. Soc.* **1980**, *102*, 6621. (b) Williams, I. H.; Maggiora, G. M.; Schowen, R. L. *J. Am. Chem. Soc.* **1980**, *102*, 7831. (c) Williams, I. H.; Spangler, D.; Femec, D. A.; Maggiora, G. M.; Schowen, R. L. *J. Am. Chem. Soc.* **1983**, *105*, 31.

(13) (a) Sherer, E. C.; Turner, G. M.; Shields, G. C. *Int. J. Quantum Chem. Quantum Biol. Symp.* **1995**, *22*, 83. (b) Turner, G. M.; Sherer, E. C.; Shields, G. C. *Int. J. Quantum Chem. Quantum Biol. Symp* **1995**, *22*, 103.

(14) (a) Sherer, E. C.; Turner, G. M.; Lively, T. N.; Landry, D. W.; Shields, G. C. *J. Mol. Model.* **1996**, *2*, 62. (b) Sherer, E. C.; Yang, G.; Turner, G. M.; Shields, G. C.; Landry, D. W. *J. Phys. Chem. A* **1997**, *101*, 8526.

(15) Zhan, C.-G.; Landry, D. W.; Ornstein, R. L. *J. Am. Chem. Soc*. **2000**, *122*, 1522.

(16) Zhan, C.-G.; Landry, D. W.; Ornstein, R. L. *J. Am. Chem. Soc*. **2000**, *122*, 2621.

(17) (a) Fersht, A. *Enzyme Structure and Mechanism*; Freeman: San Francisco, 1977. (b) Jencks, W. P. *Catalysis in Chemistry and Enzymology*; Dover Publications: New York, 1987.

(18) (a) Ecobichon, D. J. In *Casarett & Doull's Toxicology*, 5th ed.; Klaassen, C. D., Ed.; McGraw-Hill: New York, 1996; pp 643. (b) Dugas, H. *Bioorganic Chemistry*, 3rd ed.; Springer: New York, 1996.

(19) (a) Landry, D. W.; Zhao, K.; Yang, G. X.-Q.; Glickman, M.; Georgiadis, T. M. *Science* **1993**, *259*, 1899. (b) Yang, G.; Chun, J.; Arakawa-Uramoto, H.; Wang, X.; Gawinowicz, M. A.; Zhao, K.; Landry, D. W. *J. Am. Chem. Soc*. **1996**, *118*, 5881. (c) Mets, B.; Winger, G.; Cabrera, C.; Seo, S.; Jamdar, S.; Yang, G.; Zhao, K.; Briscoe, R. J.; Almonte, R.; Woods, J. H.; Landry, D. W. *Proc. Natl. Acad. Sci. U.S.A.* **1998**, *95*, 10176.

(20) (a) Weiner, S. J.; Singh, U. C.; Kollman, P. A. *J. Am. Chem. Soc*. **1985**, *107*, 2219. (b) Madura, J. D.; Jorgensen, W. L. *J. Am. Chem. Soc*. **1986**, *108*, 2517. (c) Lipez, X.; Dejaegere, A.; Karplus, M. *J. Am. Chem. Soc*. **1999**, *121*, 5548. (d) Bakowies, D.; Kollman, P. A. *J. Am. Chem. Soc*. **1999**, *121*, 5712.

(21) Cramer, C. J.; Truhlar, D. G. *J. Comput. Chem*. **1992**, *13*, 1089.

(22) Fairclough, R. A.; Hinshelwood, C. N. *J. Chem. Soc.* **1937**, 538.

(23) (a) Tomasi, J.; Persico, M. *Chem. Rev*. **1994**, *94*, 2027. (b) Cramer, C. J.; Truhlar, D. G. In *Solvent Effects and Chemical Reactions*; Tapia, O., Bertran, J., Eds.; Kluwer: Dordrecht, The Netherlands, 1996; p 1. (c) Cramer, C. J.; Truhlar, D. G. *Chem. Rev*. **1999**, *99*, 2161. (d) Chipman, D. M. *J. Chem. Phys.* **1997**, *106*, 10194. (e) Chipman, D. M. *J. Chem. Phys.* **1999**, *110*, 8012. (f) Chipman, D. M. *J. Chem. Phys.* **2000**, *112*, 5558.

(24) (a) Miertus, S.; Scrocco, E.; Tomasi, J. *Chem. Phys*. **1981**, *55*, 117. (b) Miertus, S.; Tomasi. J. *Chem. Phys.* **1982**, *65*, 239. (c) Cossi, M.; Barone, V.; Cammi, R.; Tomasi, J. *Chem. Phys. Lett.* **1996**, *255*, 327.

(25) (a) Cances, M. T.; Mennucci, B.; Tomasi, J. *J. Chem. Phys*. **1997**, *107*, 3032. (b) Cossi, M.; Barone, V.; Mennucci, B.; Tomasi, J. *Chem. Phys. Lett.* **1998**, *286*, 253. (c) Mennucci, B.; Cammi, R.; Tomasi, J. *J. Chem. Phys.* **1998**, *109*, 2798.

(26) Barone, V.; Cossi, M. *J. Phys. Chem. A* **1998**, *102*, 1995.

(27) Frisch, M. J.; Trucks, G. W.; Schlegel, H. B.; Scuseria, G. E..; Robb, M. A.; Cheeseman, J. R.; Zakrzewski, V. G.; Montgomery, J. A.; Stratmann, R. E.; Burant, J. C.; Dapprich, S.; Millam, J. M.; Daniels, A. D.; Kudin, K. N.; Strain, M. C.; Farkas, O.; Tomasi, J.; Barone, V.; Cossi, M.; Cammi, R.; Mennucci, B.; Pomelli, C.; Adamo, C.; Clifford, S.; Ochterski, J.; Petersson, G. A.; Ayala, P. Y.; Cui, Q.; Morokuma, K.; Malick, D. K.; Rabuck, A. D.; Raghavachari, K.; Foresman, J. B.; Cioslowski, J.; Ortiz, J. V.; Stefanov, B. B.; Liu, G.; Liashenko, A.; Piskorz, P.; Komaromi, I.; Gomperts, R.; Martin, R. L.; Fox, D. J.; Keith, T.; Al-Laham, M. A.; Peng, C. Y.; Nanayakkara, A.; Gonzalez, C.; Challacombe, M.; Gill, P. M. W.; Johnson, B.; Chen, W.; Wong, M. W.; Andres, J. L.; Gonzalez, A. C.; Head-Gordon, M.; Replogle, E. S.; Pople, J. A. *Gaussian 98*, Revision A6; Gaussian, Inc.: Pittsburgh, PA, 1998.

(28) (a) Zhan, C.-G.; Bentley, J.; Chipman, D. M. *J. Chem. Phys.* **1998**, *108*, 177. (b) Zhan, C.-G.; Chipman, D. M. *J. Chem. Phys.* **1998**, *109*, 10543. (c) Zhan, C.-G.; Chipman, D. M. *J. Chem. Phys.* **1999**, *110*, 1611. (d) Regarding the detail of the SVPE computation on a given solute under a given quantum mechanical approximation level, once the solute cavity is defined and the dielectric constant is know, the accuracy of the SVPE numerical computation depends only on the number of surface nodes (N) representing the cavity surface and number of layers (M) describing the volume polarization charge distribution within a certain, sufficiently large three-dimensional space outside the solute cavity. If one could use infinite number of nodes and infinite number of layers, then the numerical results obtained from the SVPE computation would be exactly the same as those determined by the exact solution of the Poisson's equation for describing the solvent polarization potential. We have shown that the accuracy of the SVPE numerical computations employed in this study with $N = 590$ and $M = 40$ (for a step of 0.3 Å) are higher than that required for obtaining Tables 1 and 2 in this paper.

(29) Zhan, C.-G.; Norberto de Souza, O.; Rittenhouse, R.; Ornstein, R. L. *J. Am. Chem. Soc.* **1999**, *121*, 7279.

(30) Schmidt, M. W.; Baldridge, K. K.; Boatz, J. A.; Elbert, S. T.; Gordon, M. S.; Jensen, J. H.; Koseki, S.; Matsunaga, N.; Nguyen, K. A.; Su, S. J.; Windus, T. L.; Dupuis, M.; Montgomery, J. A. *J. Comput. Chem.* **1993**, *14*, 1347.

(31) (a) Becke, A. D. *J. Chem. Phys*. **1993**, *98*, 5648. (b) Lee, C.; Yang, W.; Parr, R. G. *Phys. Rev. B* **1988**, *37*, 785.

(32) Frisch, M. J.; Trucks, G. W.; Schlegel, H. B.; Gill, P. M. W.; B. G. Johnson, B. G.; Robb, M. A.; Cheeseman, J. R.; Keith, T.; Petersson, G. A.; Montgomery, J. A.; Raghavachari, K.; Al-Laham, M. A.; Zakrzewski, V. G.; Ortiz, J. V.; Foresman, J. B.; Cioslowski, J.; Stefanov, B. B.; Nanayakkara, A.; Challacombe, M.; Peng, C. Y.; Ayala, P. Y.; Chen, W.; Wong, M. W.; Andres, J. L.; Replogle, E. S.; Gomperts, R.; Martin, R. L.; Fox, D. J.; Binkley, J. S.; Defrees, D. J.; Baker, J.; Stewart, J. P.; Head-Gordon, M.; Gonzalez, C.; Pople, J. A. *Gaussian 94*, Revision D.1; Gaussian, Inc.: Pittsburgh, PA, 1995.

(33) Humphreys, H. M.; Hammett, L. P. *J. Am. Chem. Soc.* **1956**, *78*, 521.

(34) Amis, E. S.; Siegel, S. *J. Am. Chem. Soc*. **1950**, *72*, 674.

(35) Schaefgen, J. R. *J. Am. Chem. Soc*. **1948**, *70*, 1308.

(36) Rylander, P. N.; Tarbell, D. S. *J. Am. Chem. Soc*. **1950**, *72*, 3021.